

MAJID ARABAMERI<sup>1</sup>, ALLAHBAKHS JAVID<sup>2</sup>, ALIAKBAR ROUDBARI<sup>3</sup>

## ARTIFICIAL NEURAL NETWORK (ANN) MODELING OF COD REDUCTION FROM LANDFILL LEACHATE BY THE ULTRASONIC PROCESS

In the study, the use of an artificial neural network (ANN) has been applied for the prediction of COD removal from landfill leachate by the ultrasonic process. The configuration of the backpropagation neural network giving the lowest mean square error (MSE) was a three-layer ANN with a tangent sigmoid transfer function (tansig) at a hidden layer with 14 neurons, linear transfer function (purelin) at the output layer and the Levenberg–Marquardt backpropagation training algorithm (LMA). The ANN predicted results are very close to the experimental data with the correlation coefficient ( $R^2$ ) of 0.992 and the MSE of 0.000331. The sensitivity analysis showed that all studied variables (contact time, pH, ultrasound frequency and power) have strong effect on COD removal. In addition, ultrasound power is the most influential parameter with relative importance of 25.8%. The results showed that modeling neural network could effectively predict COD removal from landfill leachate by ultrasonic process.

### 1. INTRODUCTION

Increasingly affluent lifestyles, continuing industrial and commercial growth in many countries around the world in the past decade has contributed to a rapid increase in both municipal and industrial solid waste production [1]. The sanitary landfill method for the ultimate disposal of solid waste material continues to be widely accepted and used due to its economic advantages (because of lowest capital costs, no need to complementary methods and possibility to use from land and biogas) [2]. The generation of

---

<sup>1</sup>Vice-Chancellery for Food and Drug, Shahroud University of Medical Sciences, Shahroud, Iran.

<sup>2</sup>Department of Environmental Health Engineering, School of Public Health, Shahroud University of Medical Sciences, Shahroud, Iran.

<sup>3</sup>Center for Health-Related Social and Behavioral Sciences Research, Shahroud University of Medical Sciences, Shahroud, Iran, corresponding author A. Roudbari, e-mail: roodbari@shmu.ac.ir

leachate remains an inevitable consequence of the practice of waste disposal in sanitary landfills [3]. Leachate are defined as the aqueous effluent generated as a consequence of rainwater percolation through wastes, biochemical processes in waste cells and the inherent water content of wastes themselves [4]. Leachates may contain large amounts of organic matter (biodegradable, but also refractory to biodegradation), where humic-type constituents consist an important group, as well as ammonia-nitrogen, heavy metals, chlorinated organic and inorganic salts [4]. When leachate move downwards from landfill into groundwater table as a result of infiltrated precipitation, groundwater gets contaminated, likewise, if the waste is buried below the water table; groundwater becomes contaminated after leaching compounds from it [5]. Since groundwater and surface water are the source of our potable water, they should be protected from such pollutants; otherwise, the cost of treating drinking water will rise and the life of biodiversity in surface water bodies will be endangered. Since landfills and leachate production cannot be completely avoided, the only thing to do is to as much as possible reduce leachate production and treat the generated ones to eliminate or reduce the level of contamination in them to discharge consent levels before releasing to the environment (receiving water bodies) [6].

In recent years many new techniques, physicochemical, biological and combined biological with physicochemical have been proposed and tested for leachate treatment [7]. Ultrasonic, as an advanced oxidation process (AOP) can degrade pollutants not only by producing hydroxyl radicals but also by exerting thermal dissociation (pyrolysis) and shear forces [7]. Ultrasound produces strong cavitation in aqueous solution causing shock wave and reactive free radicals by the violet collapse of the capitation bubbles. These effects should contribute to the physical disruption of microbial structures and inactivation as well as the decomposition of toxic chemicals [7]. Treating of wastewater by AOPs is quite complex, since the process is influenced by several factors. Due to complexity of the process, it is difficult to be modeled and simulated using conventional mathematical modeling [8]. Artificial neural networks (ANNs) are now used in many areas of science and engineering and is considered to be a promising tool because of their simplicity towards simulation, prediction and modeling [8]. The advantages of ANN are that the mathematical description of the phenomena involved in the process is not required; less time is required for model development than the traditional mathematical models and prediction ability with limited numbers of experiments [9]. Application of ANN to solve environmental engineering problems has been reported in many articles (a NN approximation of the UNESCO equation of state of the sea water and an inversion of this equation (NN for the salinity of the seawater); for atmospheric numerical models, a NN approximation for long wave irradiative transfer code; and for wave models; and a NN approximation for the nonlinear wave–wave interaction) [10]. ANNs were applied in biological wastewater treatment and physicochemical wastewater treatment [10]. However, few studies on applications of ANN in advanced oxidation processes (AOPs) have been reported. The present work investigated the implementation

of ANN for the prediction of COD removal from landfill leachate by the ultrasonic process. The ANN modeling outputs were compared with the experimental data.

## 2. MATERIALS AND METHODS

*Materials.* Samples of landfill leachate were obtained from a municipal landfill site (over 10 years old) located in Shahrood (Semnan, Iran). All leachate samples were collected from leachate lift stations or storage tanks, stored at 3 °C, and tested within 2 days of collecting the samples. Characteristics of the leachate samples were: COD 5830 mg/dm<sup>3</sup>, BOD<sub>5</sub> 3940 mg/dm<sup>3</sup>, NH<sub>4</sub>-N 730 mg/dm<sup>3</sup> and pH 8. The ammonia nitrogen concentrations were analyzed with C<sub>203</sub> 8-parameter test meter (Hanna electronics, Co., Ltd.). pH was measured with a Benchtop pH meters (Cole-Parmer Co., Ltd). The pH meter was calibrated before each use with pH 3, 7 and 10 buffer solutions. BOD and COD were determined by the procedure outlined in Standard Methods 5210 and 5220, respectively. Reagents and standard chemicals were purchased from Hach Co., except the BOD buffer solution, which was prepared according to Standard Method 5210. BOD check standards were performed with each batch of BOD measurements. The results were considered acceptable when the value of the BOD check standard fell within the range of 198±30.5 mg/dm<sup>3</sup>. The average of the BOD check standards for the entire duration of the project was 169±29 mg/dm<sup>3</sup>, which demonstrates satisfactory results giving the inherent variability in BOD measurements. COD check standards were also performed with each batch of COD measurements. A COD standard solution of 1000 mg/dm<sup>3</sup> was diluted to 200 and 500 mg/dm<sup>3</sup> to ensure the accuracy of COD measurements. The relative difference for calibration check standards (RD<sub>cal</sub>) is defined as the absolute difference of the check standard concentration and the known concentration all divided by the known concentration. The RD<sub>cal</sub> for COD was <10% for the entire duration of the project [11].

*Experimental set-up.* A cylindrical shape Plexiglas reactor totaling a volume of 1 dm<sup>3</sup> was constructed (Fig. 1). The solution in the reactor was mixed with a magnetic stirrer, while sufficient aeration was provided by a compressor connected to a porous stone located in the bottom of the reactor. The compressor was used to ensure complete mixing in the reactor. The ultrasonic source was a Model UGMA-5000 ultrasound generator with three 30, 45 and 60 kHz transducers having a titanium probe 20 mm in diameter. The power input could be adjusted continuously from 60 to 120 W. A leachate sample of 1 dm<sup>3</sup> was sonicated in a covered cylindrical glass vessel. Aeration was supplied by a Model SALWAT air compressor. The water level inside the surrounding bath was maintained by continuous circulation of cooling water, and subsequently the temperature was maintained constant at 30±2 °C. Ferrous sulfate (FeSO<sub>4</sub>·7H<sub>2</sub>O), sulfuric acid and hydrogen peroxide (Merck, 30 wt. %) were of analytical grade.

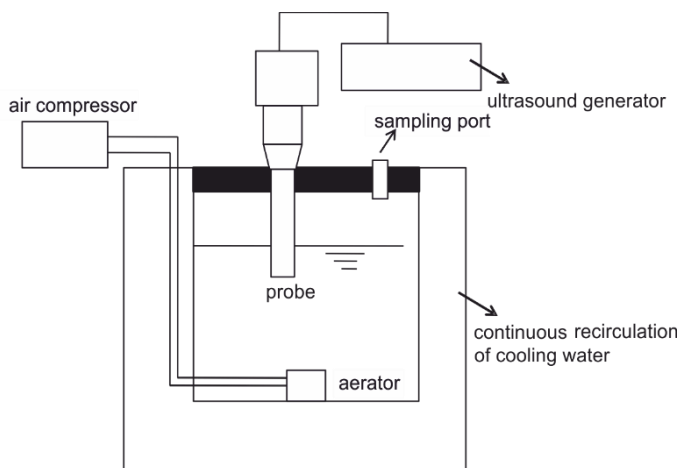


Fig. 1. Scheme of the experimental set-up

*Procedure.* After the optimization by factorial design, ultrasonic radiation was applied in the treatment of raw leachate using a batch wise mode. At first, the raw leachate sample was filtered through a 45  $\mu\text{m}$  filter paper to remove any suspended solid impurity. Then the sample was adjusted to the required pH with  $\text{H}_2\text{SO}_4$  or  $\text{NaOH}$ . Then different scenarios were tested with regard to power intensities of 70 and 110 W, frequencies of 30, 45 and 60 kHz, reaction times of 30, 60, 90 and 120 min and pH of 3, 7 and 10. COD concentration of the sonicated sample was measured by the Standard Methods 5220 based on the  $\text{K}_2\text{Cr}_2\text{O}_7$  method. pH was measured with a model Benchtop pH meters.

*Artificial neural network (ANN).* Artificial neural networks are known for their ability of learning, simulation and prediction of data [12]. Disadvantage of artificial neural network is its “black box” nature [12]. The individual relations between the input variables and the output variables are not developed by engineering judgment so that the model tends to be a black box [13]. Further there is greater computational burden and proneness to over fitting and the sample size has to be large [14]. The network consists of numerous individual processing units called neurons and commonly interconnected in a variety of structures [15]. The strength of these interconnections is determined by the weight associated with neurons. The multilayer feed-forward net is a parallel interconnected structure consisting of an input layer and includes independent variables, number of hidden layers and an output layer [15]. In this study, a three-layered back-propagation neural network with tangent sigmoid transfer function (tansig) at the hidden layer and a linear transfer function (purelin) at the output layer was used. The backpropagation algorithm was used for network training. Neural Network Toolbox V<sub>4.0</sub> of MATLAB mathematical software was used for prediction of COD removal. 216 experimental data sets were obtained from our study and were divided into training (one half), validation (one fourth) and test (one fourth) subsets, each of which contained 108, 54

and 54 samples, respectively. The input variables were reaction time ( $t$ ), pH, ultrasound frequency and power. The corresponding COD removal percent was used as a target. To ensure that all variables in the input data are important, principal component analysis (PCA) was performed as an effective procedure for the determination of input parameters [16]. It was observed that all input variables were important.

### 3. RESULTS AND DISCUSSION

#### 3.1. SELECTION OF BACKPROPAGATION TRAINING ALGORITHM

To determine the best backpropagation (BP) training algorithm, ten BP algorithms were studied. 5 neurons were used in the hidden layer as initial value for all BP algorithms. Table 1 shows a comparison of different backpropagation (BP) training algorithms. The Levenberg–Marquardt backpropagation algorithm (LMA) was able to have smaller mean square error (MSE) compared to other backpropagation algorithms [17]. Thus LMA was considered to be the best suitable training algorithm for this study.

Table 1

Comparison of 10 backpropagation algorithms with 5 neurons in the hidden layer

BP algorithm	Function	MSE	Epoch	$R^2$	Best linear equation
Levenberg–Marquardt backpropagation	trainlm	0.008	31	0.993	$y = 0.994X + 0.409$
Scaled conjugate gradient backpropagation	trainscg	0.016	98	0.986	$y = 0.984X + 0.926$
BFGS quasi-Newton backpropagation	trainbfg	0.018	58	0.985	$y = 0.987X + 0.841$
One step secant backpropagation	trainoss	0.030	30	0.976	$y = 0.959X + 2.46$
Batch gradient descent	traingd	0.486	102	0.706	$y = 0.379X + 26$
Variable learning rate back propagation	traingdx	0.449	24	0.775	$y = 0.408X + 26$
Batch gradient descent with momentum	traingdm	0.508	99	0.722	$y = 0.365X + 32.3$
Fletcher–Reeves conjugate gradient backpropagation	traingcf	0.027	26	0.978	$y = 1.05X - 0.854$
Polak–Ribiere conjugate gradient backpropagation	traingcp	0.017	102	0.985	$y = 0.985X + 1.11$
Powell–Beale conjugate gradient backpropagation	traingcb	0.020	36	0.983	$y = 0.967X + 2.25$

#### 3.2. OPTIMIZATION OF NUMBER OF NEURONS

The optimum number of neurons was determined based on the minimum value of MSE of the training and prediction set [18]. The optimization was done by using LMA as a training algorithm and varying the neuron number in the range 1–20.

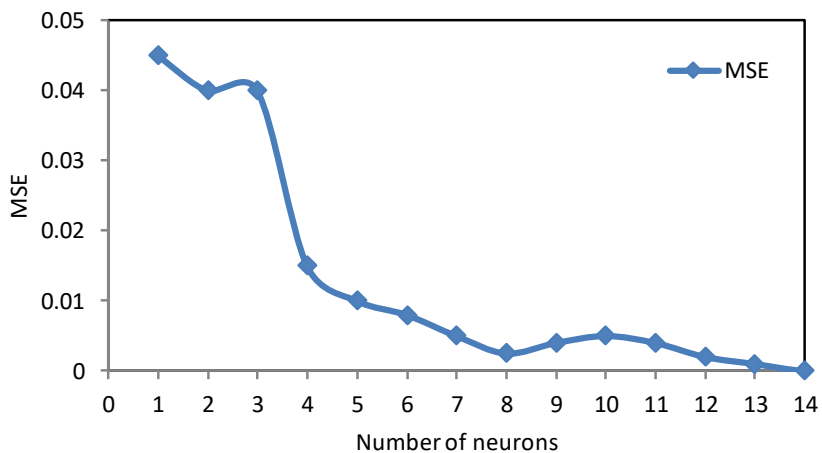


Fig. 2. Relationship between number of neurons and MSE

Figure 2 shows the relationship between number of neurons and MSE. MSE was 0.302148 when one neuron was used and decreased to 0.000331 when 14 neurons were used. Increasing the neurons to more than 14 did not significantly decrease MSE. Hence, 14 neurons were selected as the best number of neurons.

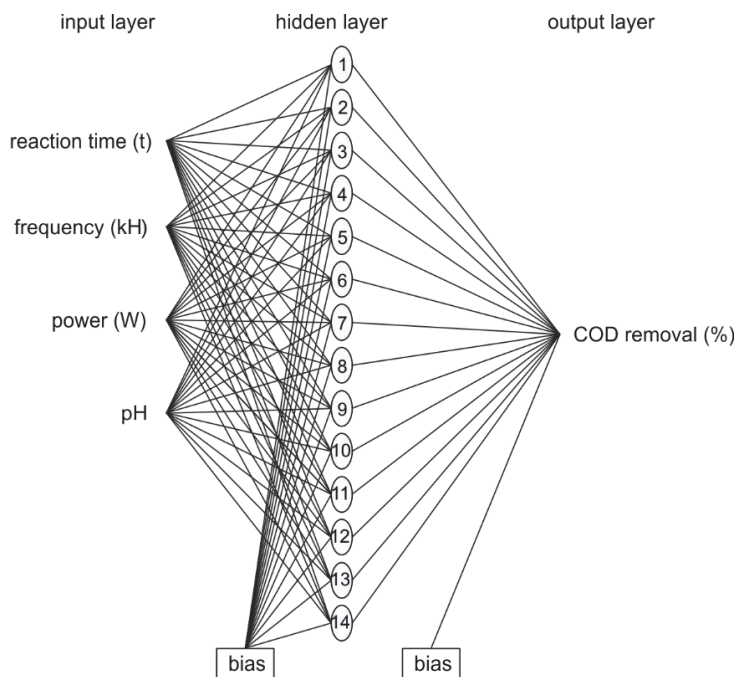


Fig. 3. Optimized ANN structure

Figure 3 shows the structure of the optimized neural network. It has three-layer ANN, with tansig function at the hidden layer with 14 neurons and a purelin function at the output layer.

### 3.3. TEST AND VALIDATION OF THE MODEL

The data sets were used to feed the optimized network in order to test and validate the model. Figure 4 shows a comparison between experimental COD removal values and predicted values using the neural network model.

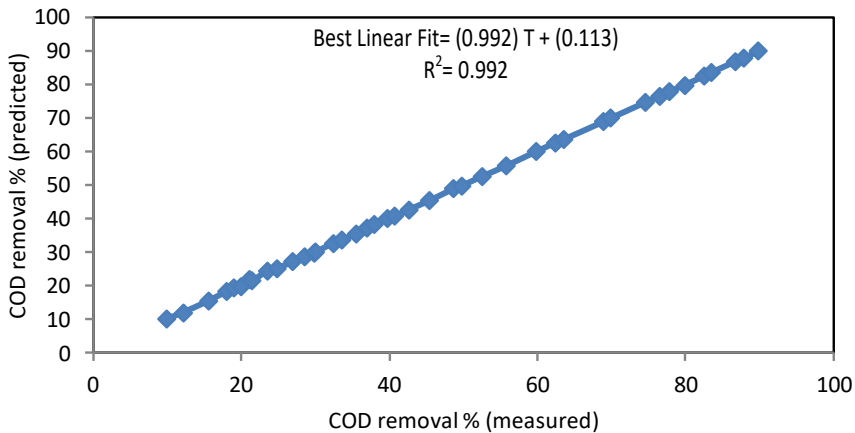


Fig. 4. COD removal. Predicted values vs. experimental ones

The best fit is indicated by a solid line with best linear equation  $A = 0.992T + 0.113$ , correlation coefficient ( $R^2$ ) 0.992 and MSE 0.000331. This agrees well with the correlation coefficient reported in the literature: the correlation coefficient of 0.985 for prediction of nitrogen oxides removal by  $\text{TiO}_2$  photocatalysis [18], 0.998 for prediction of methyl *tert*-butyl ether (MTBE) by UV/ $\text{H}_2\text{O}_2$  process [19], 0.966 for prediction of polyvinyl alcohol degradation in aqueous solution by the photo-Fenton process [20], 0.995 for removal of humic substances from the aqueous solutions by ozonation [21] and 0.98 for decolouration of Acid Orange 52 dye by UV/ $\text{H}_2\text{O}_2$  process [22].

### 3.4. SENSITIVITY ANALYSIS

In order to assess the relative importance of the input variables, two evaluation processes were used. The former one was based on the neural net weight matrix and Garson equation [23], with the partitioning of connection weights

$$I_j = \frac{\sum_{m=1}^{m=N_h} |w_{jm}^s|}{\sum_{k=1}^{k=N_i} (|W_{km}^{ih}| \times W_{mn}^{ho})} \quad (1)$$

$$\sum_{k=1}^{k=N_i} \left( \frac{\sum_{m=1}^{m=N_h} |W_{km}^{ih}|}{\sum_{k=1}^{k=N_i} |W_{km}^{ih}| \times |W_{mn}^{ho}|} \right)$$

where,  $I_j$  is the relative importance of the  $j$ th input variable on the output variable,  $N_i$  and  $N_h$  are the numbers of input and hidden neurons, respectively and  $W$  is the connection weight, the superscripts  $i$ ,  $h$ , and  $o$  refer to input, hidden and output layers, respectively, while subscripts  $k$ ,  $m$ , and  $n$  refer to input, hidden and output neurons, respectively.

Table 2

Weight matrix, weights between input and hidden layers ( $W_1$ ) and weights between hidden and output layers ( $W_2$ )

Neuron	$W_1$ Input variables				$W_2$ Output
	Time	Frequency	Power	pH	COD removal
1	0.886	0.085	-0.2431	0.317	0.739
2	-2.053	-2.053	0.891	-2.153	1.945
3	0.199	-0.091	0.211	0.013	-1.428
4	0.004	0.645	-0.782	-0.483	0.836
5	1.176	0.792	1.051	0.041	-0.767
6	-0.665	-1.187	0.754	0.054	-0.563
7	-0.807	-1.010	-1.035	0.556	-0.970
8	-0.631	-0.250	0.477	-0.584	-1.022
9	0.474	0.238	0.627	-0.261	-1.073
10	-0.865	0.445	0.497	0.965	-0.161
11	-0.913	-0.441	-1.432	0.107	-1.425
12	0.479	-0.052	0.248	0.211	-1.012
13	0.351	0.024	-0.517	-0.400	-0.371
14	0.532	1.289	1.018	1.518	1.321

Table 2 shows the weights between artificial neurons produced by the ANN model used in this work. Table 3 shows the relative importance of the input variables calculated by Eq. (1). All variables have strong effect on COD removal. The power appears to be the most influential variable followed by frequency, time and pH. The other evaluation process is based on the possible combination of variables. Performances of the groups



Table 3

Relative importance of the input variables

Input variable	Importance [%]
Time	17.6
Frequency	30.2
Power	38.2
pH	14

of one, two, three and four variables were examined by the optimal ANN structure using the LMA with 14 hidden neurons. The input variables were  $p_1$  (contact time),  $p_2$  (frequency),  $p_3$  (power) and  $p_4$  (pH).

Table 4

Evaluation of possible combinations of input variables

Combination	MSE	Epoch	$R^2$	Best linear equation
$p_1$	363.211	7	0.326	$y = 3.462X + 765$
$p_2$	270.211	8	0.578	$y = 7.692X + 810$
$p_3$	265.341	12	0.632	$y = 8.621X + 642$
$p_4$	0.563	8	0.325	$y = 3.521X + 871$
$p_1 + p_2$	0.589	14	0.564	$y = 1.84X + 689$
$p_1 + p_3$	0.521	9	0.612	$y = 0.752X + 32.1$
$p_1 + p_4$	0.391	7	0.498	$y = 0.541X + 20.1$
$p_2 + p_3$	0.304	10	0.534	$y = 0.637X - 25.6$
$p_2 + p_4$	0.456	5	0.654	$y = 0.742X + 22.8$
$p_3 + p_4$	0.489	5	0.598	$y = 0.652X + 19.6$
$p_1 + p_2 + p_3$	0.189	6	0.823	$y = 0.614X + 16.3$
$p_1 + p_2 + p_4$	0.175	9	0.795	$y = 0.567X + 25.3$
$p_2 + p_3 + p_4$	0.116	10	0.758	$y = 0.741X + 11.4$
$p_1 + p_2 + p_3 + p_4$	0.132	6	0.699	$y = 0.687X + 16$

Table 4 shows the results of the sensitivity analysis for different combinations of input variables. The sensitivity analysis showed that  $p_3$  was the most effective parameter among other variables in the group of one variable. The MSE (265.341) decreased up 0.304, which is the minimum value of the group of two variables when  $p_3$  was used in combination with  $p_2$ . The MSE (0.304) decreased up to 0.116, which is the minimum value of the group of three variables when  $p_2$  was used in combination with  $p_3$  and  $p_4$ . The best group performances according to number of parameters are shown in Table 4. MSE values decreased as the number of variables in the group increased due to the contribution of all parameters. It can be concluded that the power is the most effective parameter. In addition, all variables have strong effect on COD removal and it agrees well with the sensitivity analysis using Garson equation.

## 3.5. EFFECT OF pH

The pH value influences the generation of hydroxyl radicals and hence the COD removal efficiency [24]. To examine the effect of pH, experiments were conducted by varying the pH in the range 3–10. An initial COD concentration was  $5830 \text{ mg/dm}^3$ . The other operating conditions were fixed at power 70 W and frequency 30 kHz.

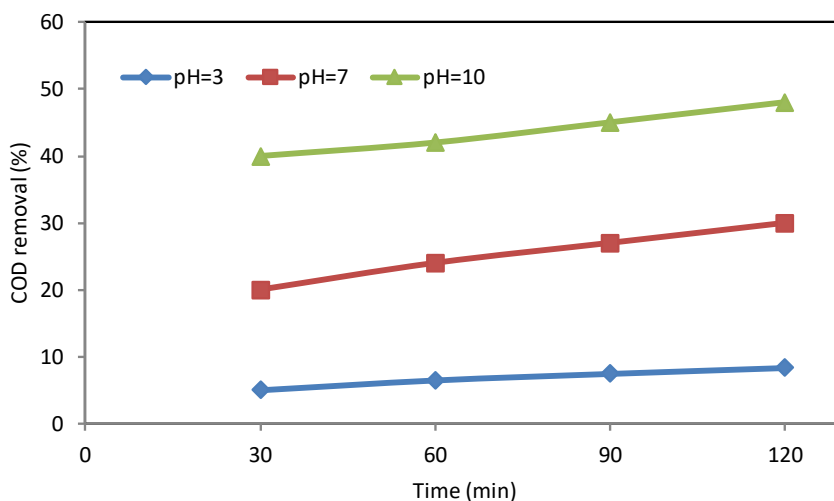


Fig. 5. Effect of initial pH on the COD removal

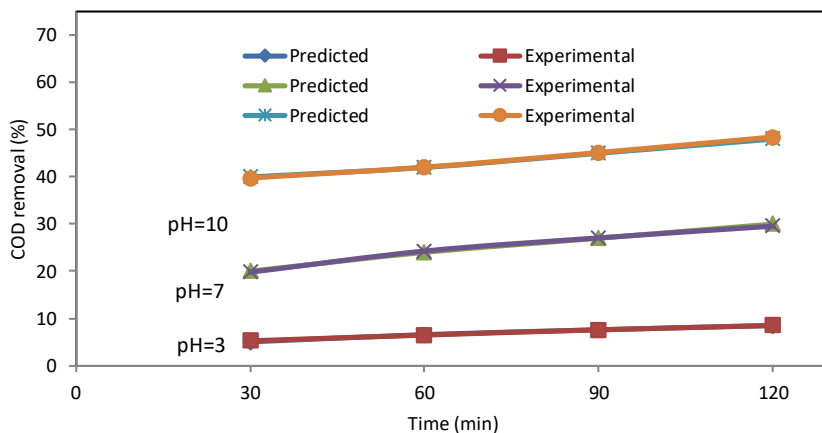


Fig. 6. Comparison between ANN output and experimental results at various pH

The results (Fig. 5) show that pH significantly influences COD removal. Decrease in COD removal at pH lower than 3 may be due to the decrease in dissolved iron and oxidation rate [24]. Further, hydrogen peroxide is stable at low pH presumably because

it gets solvated in the presence of high concentration of  $H^+$  to form stable oxonium ions ( $H_3O_2^+$ ), thus reducing substantially its reactivity with ferrous ions [25]. Therefore, the number of hydroxyl radicals would decrease at low pH, decreasing degradation of antibiotic intermediates. In terms of the relation between the experimental results and the predicted values of COD removal by the model, Fig. 6 shows that predicted values are in good agreement with the experimental results.

### 3.6. EFFECT OF CONTACT TIME

To examine the effect of contact time on COD removal, the contact time was varied in the range 30–120 min at constant initial COD of  $5830 \text{ mg/dm}^3$ . The other operating conditions were fixed at pH 7, power 110 W and frequency 45 kHz. The corresponding COD removal was 61, 70, 78, and 88% (Fig. 7).

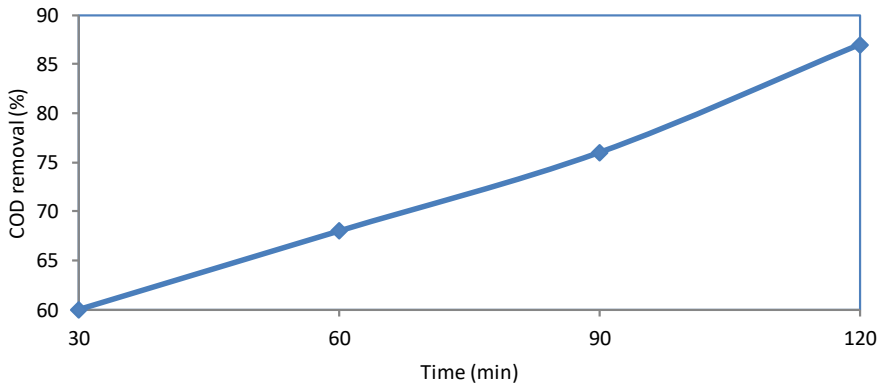


Fig. 7. Effect of contact time on COD removal

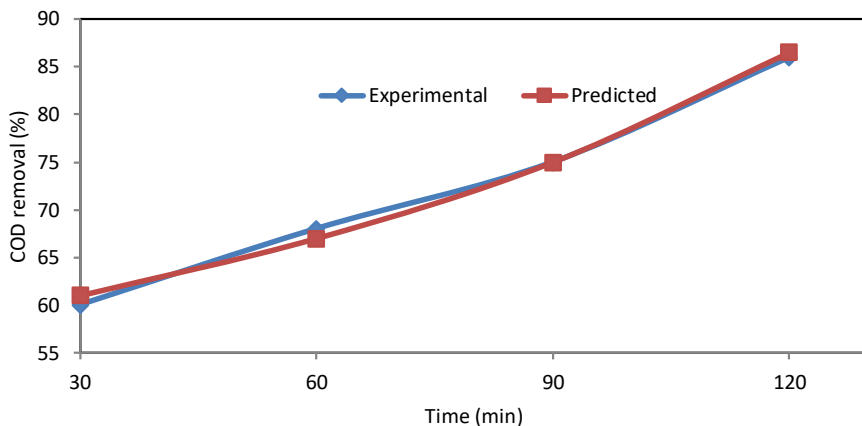


Fig. 8. Comparison of time dependences of ANN output and experimental results

Figure 8 shows a comparison between the predicted and experimental values of COD removal at various contact times. The results show that contact time increases COD removal due to the increase of contact between hydroxyl radicals and organic matter [25].

### 3.7. EFFECT OF ULTRASOUND POWER AND FREQUENCY

Figure 9 shows the effect of ultrasound power on the COD removal. The power value influences the energy of hot spots and cavitations and hence the removal efficiency [25]. To examine the effect of power, experiments were conducted by varying the powers in the range of 70–110 W. An initial COD concentration was  $5830 \text{ mg/dm}^3$ . The other operating conditions were fixed at the pH 7 and frequency 45 kHz. Figure 10 shows a comparison between the predicted and experimental values of COD removal at various power values.

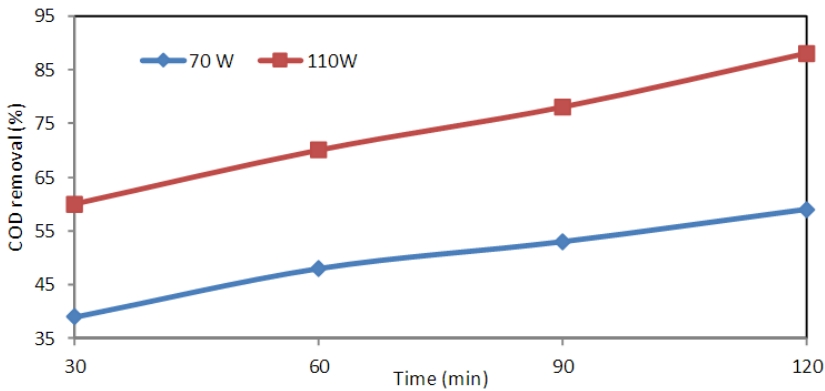


Fig. 9. Effect of power input on COD removal

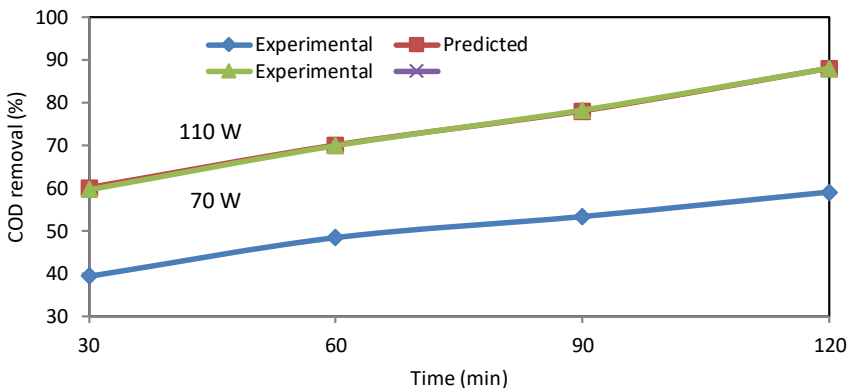


Fig. 10. Comparison between ANN output and experimental results at different powers

The frequency value influences the number of hot spots and cavitations energy and hence the removal efficiency [25]. To examine the effect of frequency, experiments were conducted by varying the frequency in the range of 30–60 kHz. An initial COD concentration was  $5830 \text{ mg/dm}^3$ . The other operating conditions were fixed at the pH 7 and power 110 W. Figure 11 shows a comparison between the predicted and experimental values of COD removal at different frequencies.

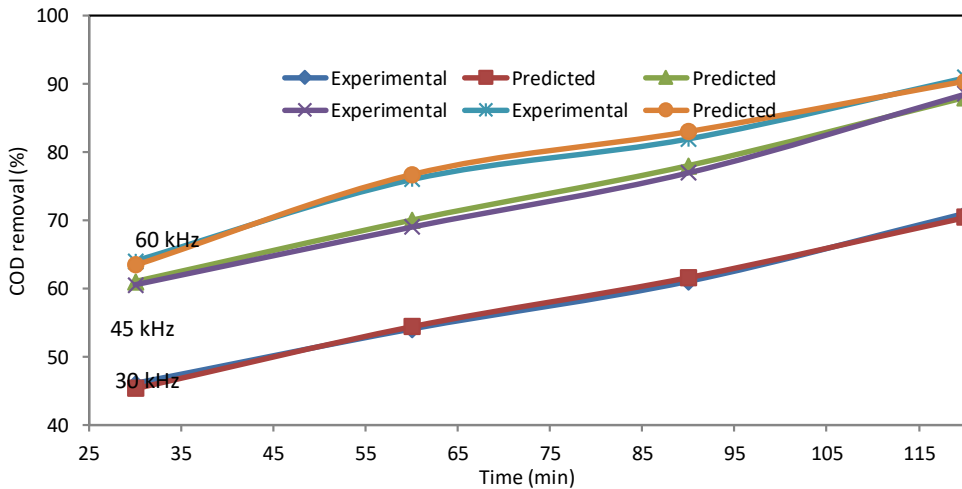


Fig. 11. ANN output and experimental results at various frequencies

#### 4. CONCLUSIONS

A three-layer back propagation neural network was optimized to predict the COD removal from landfill leachate by the ultrasonic process. The configuration of the back propagation neural network giving the smallest MSE was three-layer ANN with a tangent sigmoid transfer function (tansig) at a hidden layer with 14 neurons, a linear transfer function (purelin) at the output layer, and the Levenberg–Marquardt back propagation training algorithm (LMA). ANN predicted results are very close to the experimental ones with the correlation coefficient ( $R^2$ ) of 0.992 and MSE 0.000331. The sensitivity analysis showed that all studied variables (contact time, power, frequency and pH) have strong effect on COD removal. In addition, power is the most influential parameter of the relative importance of 39.2%. ANN results showed that neural network modeling could effectively predict the behavior of the process.

The results showed that AOP process for COD removal from landfill leachate can be replaced with ANN in which mathematical description of the phenomena involved in the process is not required; less time is required for model development than the

traditional mathematical models and prediction ability with limited numbers of experiments is possible.

#### ACKNOWLEDGEMENT

The authors are grateful to the management and authorities of the research affairs of Shahroud University of Medical Sciences for providing facilities for this research.

#### REFERENCES

- [1] MAHVI A., ROUDBARI A., NABIZADEH R., NASERI S., DEGHANI M., ALIMOHAMMADI M., *Improvement of landfill leachate biodegradability with ultrasonic process*, Eur. J. Chem., 2012, 9, 766.
- [2] MAHVI A., ROUDBARI A., *Survey on the effect of landfill leachate of Shahroud city of Iran on ground water Quality*, J. Appl. Technol. Environ. San., 2011, 1, 17.
- [3] RENOU S., GIVAUDAN J., POULAIN S., DIRASSOUYAN F., MOULIN P., *Landfill leachate treatment: review and opportunity*, J. Hazard. Mater., 2008, 150, 468.
- [4] RAJAN G., NALLADURAI D., PUTHIVA N., SREEKRISHNAPERUMAL R., SUBRAMANIAM K., *Use of combined coagulation process as pre-treatment of landfill leachate*, Ir. J. Environ. Health Sci. Eng., 2013, 10, 24.
- [5] SAMADI T., ESFAHANI Z., NADDAFI K., *Comparison of the efficacy of Fenton and nZVI + H<sub>2</sub>O<sub>2</sub> processes in municipal solid waste landfill leachate treatment. Ccase study: Hamadan landfill leachate*, Int. J. Environ. Res., 2013, 7, 187.
- [6] ABDOLI A., KARBASSI R., SAMIEE-ZAFARGHANDI R., RASHIDI Z., GITIPOUR S., PAZOKI M., *Electricity generation from leachate treatment plant*, Int. J. Environ. Res., 2012, 7, 493.
- [7] ZHA G., ZHANG X., XU C., *Treatment of landfill leachate by sonolysis followed by fenton process*, Desalination Water. Treat., 2013, 1.
- [8] ALEBOYEH A., KASIRI B., OLYA E., ALEBOYEH H., *Prediction of azo dye decolorization by UV/H<sub>2</sub>O<sub>2</sub> using artificial neural networks*, Dyes Pigments, 2008, 77, 288.
- [9] YETILMEZSOY K., DEMIREL S., *Artificial neural network (ANN) approach for modeling of Pb(II) adsorption from aqueous solution by Antep pistachio (Pistacia Vera L.) shells*, J. Hazard. Mater., 2008, 153, 1288.
- [10] OGUZA E., TORTUM A., KESKINLER B., *Determination of the apparent rate constants of the degradation of humic substances by ozonation and modeling of the removal of humic substances from the aqueous solutions with neural network*, J. Hazard. Mater., 2008, 157, 455.
- [11] FULAZZAKY A., *Measurement of biochemical oxygen demand of the leachates*, Environ. Monit. Assess., 2013, 185, 4721.
- [12] GUIMARAES C., FILHO R., SIQUEIRA F., FILHO I., SILVA B., *Optimization of the AZO dyes decoloration process through neural networks: determination of the H<sub>2</sub>O<sub>2</sub> addition critical point*, Chem. Eng. J., 2008, 141, 35.
- [13] ELMOLLAA S., CHAUDHURIA M., ELTOUKHY M., *The use of artificial neural network (ANN) for modeling of COD removal from antibiotic aqueous solution by the Fenton process*, J. Hazard. Mater., 2010, 179, 127.
- [14] SINGH P., BASANT A., MALIK A., JAIN G., *Artificial neural network modeling of the river water quality. A case study*, Ecol. Model., 2009, 220, 888.
- [15] MJALLI S., AL-ASHEH S., ALFADALA E., *Use of artificial neural network black-box modeling for the prediction of wastewater treatment plants performance*, J. Environ. Manage., 2007, 83, 329.

- 
- [16] HERNANDEZ RAMIREZ A., HERRERA-LÓPEZ J., RIVERA L., REAL-OLVERA D., *Artificial neural network modeling of slaughterhouse wastewater removal of COD and TSS by electrocoagulation*, Stud. Fuzz. Soft. Comp., 2014, 312, 273.
- [17] VYAS M., MODHERAB B., SHARMA K., *Artificial neural network based model in effluent treatment process*, Int. J. Adv. Engine. Technol., 2011, 2, 271.
- [18] TURAN G., MESCI B., OZGONENEL O., *The use of artificial neural networks (ANN) for modeling of adsorption of Cu (II) from industrial leachate by pumice*, Chem. Eng. J., 2011, 171, 1091.
- [19] WANG L., WU H., WANG S., LI F., TAO J., *Removal of organic matter and ammonia nitrogen from landfill leachate by ultrasound*, Ultrason. Sonochem., 2008, 15, 933.
- [20] GIROTO A., GUARDANI R., TEIXEIRA C., NASCIMENTO O., *Study on the photo-Fenton degradation of polyvinyl alcohol in aqueous solution*, Chem. Eng. Proc., 2006, 45, 523.
- [21] LEGUBE B., VEL LEITNER K., *Heterogeneous photocatalytic treatment of pharmaceutical micropollutants: effects of wastewater effluent matrix and catalyst modifications*, Appl. Catal. B Environ., 2014, 147, 8.
- [22] SHU Y., CHANG C., *Decolorization effects of six azo dyes by O<sub>3</sub>, UV/O<sub>3</sub> and UV/H<sub>2</sub>O<sub>2</sub> processes*, Dyes. Pigments, 2005, 65, 25.
- [23] MHURCHÚ N., FOLEY G., *Dead-end filtration of yeast suspensions: correlating specific resistance and flux data using artificial neural networks*, J. Memb. Sci., 2006, 281, 325.
- [24] CHEN S., SUN D., CHUNG S., *Simultaneous removal of COD and ammonium from landfill leachate using an anaerobic-aerobic moving-bed biofilm reactor system*, Waste Manage., 2008, 28, 339.
- [25] KURNIAWAN A., LO H., CHAN G., SILLANPÄÄ T., *Biological processes for treatment of landfill leachate*, J. Environ. Monit., 2010, 12, 2032.